Effects of Lipid Phase Transition and Membrane Surface Charge on the Interfacial Activation of Phospholipase A_2

Supriyo Ray, Jennifer L. Scott, and Suren A. Tatulian*

Biomolecular Science Center, Burnett College of Biomedical Sciences, University of Central Florida, 12722 Research Parkway, Orlando, Florida 32826

Received July 28, 2007; Revised Manuscript Received September 11, 2007

ABSTRACT: Phospholipase A_2 (PLA_2) enzymes act at the membrane−water interface to access their phospholipid substrate from the membrane. They are regulated by diverse factors, including the membrane charge, fluidity, mode of membrane binding (insertion, orientation), and allosteric conformational effects. Relative contributions of these factors to the complex kinetics of PLA_2 activation are not well understood. Here we examine the effects of thermal phase transitions and the surface charge of phospholipid membranes on the activation of human pancreatic PLA_2. The temperature dependence of the initial catalytic rate of PLA_2 peaks around the lipid phase transition temperature (T_m) when T_m is not too far from physiological temperatures (30−40 °C), and the peak is higher in the presence of anionic membranes. High PLA_2 activity can be induced by thermal perturbations of the membrane. Temperature-dependent fluorescence quenching experiments show that despite dramatic effects of the lipid phase transition on PLA_2 activity, the membrane insertion depth of PLA_2 increases only modestly above T_m. The data show that membrane structural disorder, and not the depth of membrane insertion, plays a major role in PLA_2 activity.

Secreted phospholipase A_2 (PLA_2)[1] enzymes hydrolyze glycerophospholipids to lysophospholipids and free fatty acids and are involved in various normal and pathological processes such as lipid metabolism and inflammation (*1*−*3*). They are typical interfacial enzymes that reach their full activity when they bind to cellular membranes and undergo interfacial activation (*4*). Electrostatic and nonpolar forces, including desolvation and entropic components, have been identified as the major factors in PLA_2−membrane interactions, which eventually result in enzyme activation (*5*−*7*). There is solid evidence that membrane binding itself is necessary but not sufficient for the interfacial activation. Under certain circumstances these enzymes demonstrate a dormant latency period before activation, which results in complex kinetics of PLA_2 activity that depends on numerous factors, such as membrane charge, thermal phase transitions, the presence of reaction products, and membrane structural features (*6*, *8*−*15*).

Complicated results have been reported regarding relationships among lipid phase transitions, PLA_2 binding, the lag phase, and activation. Jain et al. (*16*) reported that porcine group IB PLA_2 (pIBPLA$_2$), unlike a cobra venom (group IA) PLA_2, did not bind to the pure ditetradecylphosphatidylcholine membranes at temperatures below or above the lipid gel-to-fluid phase transition temperature (T_m), but did bind to membranes over a wide temperature range when reaction products were added. The activity of pIBPLA$_2$ against 1,2-dipalmitoyl-*sn*-glycero-3-phosphocholine (DPPC) vesicles increased near T_m of this lipid and was substantially higher against 1-palmitoyl-2-oleoyl-*sn*-glycero-3-phosphocholine (POPC) than DPPC vesicles at all temperatures tested, which was interpreted in terms of easier penetration of the enzyme into more fluid membranes (*9*). Data obtained in a different laboratory indicated that the same pIBPLA$_2$ efficiently hydrolyzed DPPC vesicles at temperatures below but not above T_m, although when the temperature of the vesicle−PLA_2 sample was rapidly increased to $T \geq T_m$, high enzyme activity was detected (*17*). These latter data were rationalized by effective binding of PLA_2 to the membranes in the gel phase as a prerequisite of PLA_2 activation. While membrane binding of a viper venom group IIA PLA_2 was found to weaken above T_m (*18*, *19*), a dimeric group IIA PLA_2 was shown to preferentially bind to and hydrolyze fluid membranes or the fluid domains in membranes of binary zwitterionic lipids (*20*). Although apparent inconsistencies in these studies may be attributed to differences in experimental conditions, methods, and PLA_2 isoforms, they remain largely unresolved and require detailed analysis of thermal effects in PLA_2 activation.

Despite extensive efforts toward understanding the possible role of membrane insertion of PLA_2 in enzyme activation,

* To whom correspondence should be addressed. Phone: (407) 882-2260. Fax: (407) 384-2062. E-mail: statulia@mail.ucf.edu.

[1] Abbreviations: bisPyPC 1,2-bis(1-pyrenedecanoyl)-*sn*-glycero-3-phosphocholine; Br_2PC, 1-palmitoyl-2-stearoyldibromo-*sn*-glycero-3-phosphocholine; DMPC, 1,2-dimyristoyl-*sn*-glycero-3-phosphocholine; DMPG, 1,2-dimyristoyl-*sn*-glycero-3-phosphoglycerol; DPPC, 1,2-dipalmitoyl-*sn*-glycero-3-phosphocholine; DPPG, 1,2-dipalmitoyl-*sn*-glycero-3-phosphoglycerol; DSPC, 1,2-distearoyl-*sn*-glycero-3-phosphocholine; DSPG, 1,2-distearoyl-*sn*-glycero-3-phosphoglycerol; GP, generalized polarization; hIBPLA$_2$, human group IB phospholipase A_2; laurdan, 6-lauroyl-2-(*N*,*N*-dimethylamino)naphthalene; LUV, large unilamellar vesicle; PC, phosphatidylcholine; PG, phosphatidylglycerol; PLA_2, phospholipase A_2; pIBPLA$_2$, porcine group IB phospholipase A_2; POPC, 1-palmitoyl-2-oleoyl-*sn*-glycero-3-phosphocholine; POPG, 1-palmitoyl-2-oleoyl-*sn*-glycero-3-phosphoglycerol; RET, resonance energy transfer.

10.1021/bi7015102 CCC: $37.00
Published on Web 10/18/2007

no consensus has yet been achieved. Early EPR and other data suggested that partial membrane insertion was necessary for efficient membrane binding and activity of pIBPLA$_2$ (*21*, *22*). The results of molecular dynamics analysis yielded two models of a membrane-bound human group IIA PLA$_2$, one with insignificant membrane insertion corresponding to a low activity state and the other with deeper insertion corresponding to a high activity state of the enzyme (*23*). This echoes with the idea of two membrane binding modes of PLA$_2$, formulated by Biltonen and colleagues (*5*, *24*), which proposes that transition of membrane-bound PLA$_2$ from one binding mode to another, probably involving deeper membrane insertion, contributes to interfacial activation. Consistent with this model, a recent neutron reflection and ellipsometry study on pIBPLA$_2$ and a cobra venom PLA$_2$ suggested that the membrane insertion increases during the lag phase and reaches a *catalytic depth* that results in onset of high PLA$_2$ activity (*15*). These conjectures are in line with an earlier notion that "bilayer penetration may be linked to the concept of interfacial activation" of secreted PLA$_2$'s (*9*).

On the other hand, Jain and co-workers have argued that the mechanism of the onset of high PLA$_2$ activity that follows the lag phase is the product-mediated enhancement in membrane binding affinity rather than membrane insertion of PLA$_2$ (*8*, *25*). The key objection against membrane insertion has been the idea that this would require energetically unfavorable distortion of the structure of membrane lipids (*25*). Irrespective of any logical arguments, the issue can be resolved strictly on the basis of experimental data. Significant membrane penetration of human group IB PLA$_2$ (hIBPLA$_2$) and a V3W mutant of human group IIA PLA$_2$ has been identified (*26*, *27*). However, detailed analysis of the temperature dependence of PLA$_2$ activity and correlation with membrane insertion has not been carried out. Therefore, here we conduct analysis of the temperature dependence of the activity of hIBPLA$_2$ against phospholipid membranes with T_m varying in a wide range and in parallel determine membrane insertion of PLA$_2$ as a function of temperature. The data indicate that despite the strong effects of the lipid phase transition on hIBPLA$_2$ activity, the depth of membrane insertion of the enzyme undergoes only a moderate change at T_m. Our data show that while membrane insertion of PLA$_2$ is probably important for tight membrane anchoring, factors such as membrane structural perturbations contribute to the onset of high activity of the enzyme more significantly than the membrane insertion depth.

MATERIALS AND METHODS

Materials. The fluorescent lipids 1,2-bis(1-pyrenedecanoyl)-*sn*-glycero-3-phosphocholine (bisPyPC) and 6-lauroyl-2-(*N*,*N*-dimethylamino)naphthalene (laurdan) were purchased from Invitrogen-Molecular Probes (Eugene, OR). All other lipids, i.e., 1-palmitoyl-2-stearoyl-dibromo-*sn*-glycero-3-phosphocholines (Br$_2$PCs), POPC, 1-palmitoyl-2-oleoyl-*sn*-glycero-3-phosphoglycerol (POPG), 1,2-dimyristoyl-*sn*-glycero-3-phosphocholine (DMPC), 1,2-dimyristoyl-*sn*-glycero-3-phosphoglycerol (DMPG), DPPC, 1,2-dipalmitoyl-*sn*-glycero-3-phosphoglycerol (DPPG), 1,2-distearoyl-*sn*-glycero-3-phosphocholine (DSPC), and 1,2-distearoyl-*sn*-glycero-3-phosphoglycerol (DSPG), were from Avanti Polar Lipids (Alabaster, AL). The hIBPLA$_2$ was recombinantly expressed in *Escherichia coli* and purified as described previously (*28*). Most of the other reagents were purchased from Sigma-Aldrich (St. Louis, MO).

Vesicle Preparation. Lipid solutions in chloroform or a chloroform−methanol (2:1, v/v) mixture were combined at the desired proportions, and the solvent was evaporated under nitrogen and then by incubation under vacuum overnight. To prepare large unilamellar vesicles (LUVs), an aqueous buffer was added to the dry lipid, followed by vigorous vortexing and by extrusion through 100 nm pore-size polycarbonate membranes, using a Liposofast extruder (Avestin, Ottawa, Canada). Vortexing and extrusion were done at room temperature for vesicles composed of POPC, POPG, DMPC, DMPG, and their mixtures. For lipids with higher T_m, it was necessary to heat the suspension above T_m, e.g., to 50 °C for DPPC and DPPG and to 60 °C for DSPC and DSPG. In the latter cases, extrusion was performed with the extruder immersed in water heated to the desired temperature in a large beaker. Following extrusion, the lipid suspensions were allowed to equilibrate at room temperature for 1 h prior to the measurements.

Measurements of Lipid Phase Transitions. Lipid phase transitions were studies by measuring the generalized polarization (GP) of laurdan as a function of temperature, as well as by temperature-dependent changes in the fluorescence spectra of bisPyPC. Vesicles, incorporating 1 mol % laurdan or 2.5 mol % bisPyPC, were contained in a 4 × 4 mm^2 rectangular quartz cuvette, which was thermostated in a sample holder of a Jasco-810 spectrofluoropolarimeter (Jasco Corp., Tokyo, Japan) equipped with a Peltier temperature controller and with an additional photomultiplier tube mounted at 90° for fluorescence measurements. Laurdan was excited at 360 nm, and emission spectra were recorded between 380 and 560 nm, whereas bisPyPC was excited at 347 nm, and emission spectra were recorded between 360 and 500 nm. At temperatures $T < T_m$, when the lipid is in the gel state, tight packing of lipids minimizes water penetration into the membrane, resulting in a nonrelaxed fluorescence emission peak of laurdan around 440 nm, and at $T > T_m$ water penetration increases, giving rise to the solvent-relaxed peak around 475 nm (*29*, *30*). Values of GP were calculated at various temperatures as GP = $(F_{440} - F_{475})/(F_{440} + F_{475})$, where F_{440} and F_{475} are the fluorescence emission intensities at the respective wavelengths. The lipid phase transition from the gel to liquid crystalline state results in a sigmoidal decrease in GP with a midpoint at T_m. In bisPyPC experiments, lipid phase transition results in a sharp decrease in the difference between fluorescence intensities of pyrene monomer around 378 nm and pyrene excimer around 470 nm (see the Results for more details). The excitation and emission slits were 1 and 10 nm, respectively.

Membrane Insertion of PLA$_2$. The depth of membrane insertion was determined by using differential quenching of the fluorescence of the single Trp[3] of hIBPLA$_2$ by Br$_2$PCs, as described previously (*27*). Because 20 mol % Br$_2$PCs considerably affected the lipid phase transition, in all experiments 10 mol % Br$_2$PCs were used. The experimental data were described using a "distribution analysis" (*31*, *32*):

$$\ln \frac{F_0}{F} = \frac{S}{\sigma(2\pi)^{1/2}} \exp\left[-\frac{(h - h_m)^2}{2\sigma^2}\right] \qquad (1)$$

where F_0 and F are fluorescence intensities without and with the quencher, S is the area under the distribution curve and is directly proportional to the degree of the exposure of the fluorophore to the membrane hydrocarbon core, σ is the dispersion (the half-width at half-height) of the distribution curve and is determined by the sizes of the fluorophore and the quencher, as well as by the structural disorder and heterogeneity of the system, h is the distance from the membrane center, and h_m is the most probable location of the fluorophore with respect to the membrane center. Trp fluorescence spectra were measured in the presence of vesicles with four different lipid compositions, i.e., containing 70 mol % DMPC and 30 mol % DMPG and 60 mol % DMPC, 30 mol % DMPG, and 10 mol % Br_2PC brominated at the 6,7-, 9,10-, or 11,12-positions of the *sn*-2 chain, at a total lipid concentration of 0.8 mM in 50 mM NaCl, 1 mM EGTA, and 50 mM Hepes (pH 7.4). The final concentration of PLA_2 that was added to the suspension after preparation of the vesicles was 6 μM. Lipid and protein concentrations were selected in a way that the majority of the protein was bound to the membranes. Thus, a formalism described by Qin et al. (*28*) indicates that if the dissociation constant of hIBPLA$_2$ for membranes containing 30 mol % anionic lipid is $\sim$2 μM (*28*, *33*), then at these lipid and protein concentrations nearly 80% of all PLA_2 is bound to the membranes. Spectra of bare lipids were measured as references and used for correction by subtracting the reference spectra (without PLA_2) from the sample spectra (with PLA_2). Samples were thermostated at each temperature for 5 min before the spectra were recorded, with constant stirring by a magnetic stir bar in a 4×4 mm^2 quartz cuvette. The three values of $\ln(F_0/F)$, which were obtained with three different Br_2PCs, were plotted as a function of the distance of bromines in Br_2PCs from the membrane center, i.e., 11.0, 8.3, and 6.5 Å for 6,7-, 9,10-, and 11,12-Br_2PC (*34*). Fitting of these data by eq 1 allowed determination of the parameters S, σ, and h_m.

PLA_2 Activity Assay. PLA_2 activity was measured by a fluorescence assay, using phospholipid vesicles labeled with 2.5 mol % bisPyPC, as described previously (*35*). A fluorescence spectrum of vesicles with bisPyPC was recorded between 360 and 500 nm after equilibration of the sample at a given temperature for 8 min, using $\lambda_{exc} = 347$ nm. Immediately following addition of 1 vol % stock PLA_2 solution, resulting in a final PLA_2 concentration of 0.5 μM, a macro program was activated that measures consecutive spectra with a periodicity of 1.7 min^{-1}. All measurements were conducted with constant stirring, and in most experiments a total of 36 spectra were recorded in the presence of PLA_2. The emission spectrum of monomeric pyrene contains two peaks around 378 and 396 nm, whereas the proximity of pyrene moieties results in a strong excimer peak around 470 nm (*35*, *36*). Upon lipid hydrolysis by PLA_2 the two pyrene moieties separate from each other, resulting in a decrease in the excimer signal and increase in the monomer signal. This allows determination of the activity as $R_t/R_0 - 1$, where R_t is the ratio of fluorescence intensities at 378 and 470 nm at time t, $R_t = (F_{378}/F_{470})_t$, and R_0 is R_t before addition of PLA_2. The initial catalytic rates of PLA_2 at each temperature were obtained by averaging the first five values of $(R_t/R_0 - 1)/t$, which gives the change in $R_t/R_0 - 1$ per minute immediately following combination of PLA_2 with lipid vesicles. In cases of high PLA_2 activity, where deviations from linearity occurred at early stages of lipid hydrolysis, the first three data points were averaged. PLA_2 concentrations were determined on the basis of absorbance at 280 nm measured on a Cary 100 spectrophotometer (Varian Inc., Palo Alto, CA) using $\epsilon_{280} = 18\,910$ M^{-1} cm^{-1}.

RESULTS

Lipid Phase Transition. It has been shown previously that hIBPLA$_2$, as other cationic PLA_2 isoforms, demonstrates increased activity against membranes containing anionic lipids (*5*−*7*, *21*, *27*, *28*, *35*). To assess the effect of the membrane surface charge on PLA_2 activity, experiments have been carried out on membranes composed of 100% zwitterionic lipid, phosphatidylcholine (PC), or combinations of PC with 30 mol % or more of an anionic lipid, phosphatidylglycerol (PG). PC was chosen because it is an abundant lipid in most animal cell membranes, and PG was chosen among other anionic lipids because PC and PG with identical acyl chains have similar gel-to-fluid phase transition temperatures: T_m is -2 to -4 °C for POPC and POPG, 23.5 °C for DMPC, 24.0 °C for DMPG, 41.5 °C for both DPPC and DPPG, 55.5 °C for DSPC, and 54.5 °C for DSPG (*37*−*39*). Because of the similarity in T_m values of PC and PG with identical acyl chains, it was expected that membranes composed of appropriately selected PC and PG will undergo relatively sharp thermotropic phase transition at their common T_m. The DMPC/DMPG system was studied more extensively than other lipids because with these vesicles the effect of lipid phase transition on PLA_2 activity could be analyzed without exceeding the physiological temperature range.

The shape of fluorescence spectra of laurdan in DMPC vesicles significantly changes as a function of temperature (Figure 1A of the Supporting Information). With increasing temperature, the nonrelaxed component around 440 nm decreases and the solvent-relaxed component around 475 nm increases, resulting in a sigmoidal decrease in the values of $GP = (F_{440} - F_{475})/(F_{440} + F_{475})$ with a midpoint at T_m. The lipid phase transition is completely reversible, as demonstrated by coincident spectra obtained at heating and cooling cycles and the thermal profiles of GP shown in Figure 1A,D of the Supporting Information. Membranes made of DMPG exhibit similar behavior, and at high temperatures the spectra show better resolved relaxed and nonrelaxed components (Figure 1B of the Supporting Information). The thermal profile of GP values of DMPG is also similar to that of DMPC, with nearly identical T_m values and slightly higher values of GP at lower temperatures compared to those of DMPC (Figure 1D of the Supporting Information). This feature can be explained by stronger H-bonding between DMPG molecules at $T < T_m$ because of tighter molecular packing in the gel phase. Laurdan fluorescence spectra in membranes composed of 70 mol % DMPC and 30 mol % DMPG demonstrate features intermediate between those of DMPC and DMPG membranes, and the thermal profile of GP shows a sharp, sigmoidal phase transition with $T_m =$ 23.5 °C (heating) and 24.0 °C (cooling). (Values of T_m have been deduced from first derivatives of GP thermal profiles, not shown.)

Because PLA_2 activity at various temperatures was measured by the change in fluorescence spectra of bisPyPC,

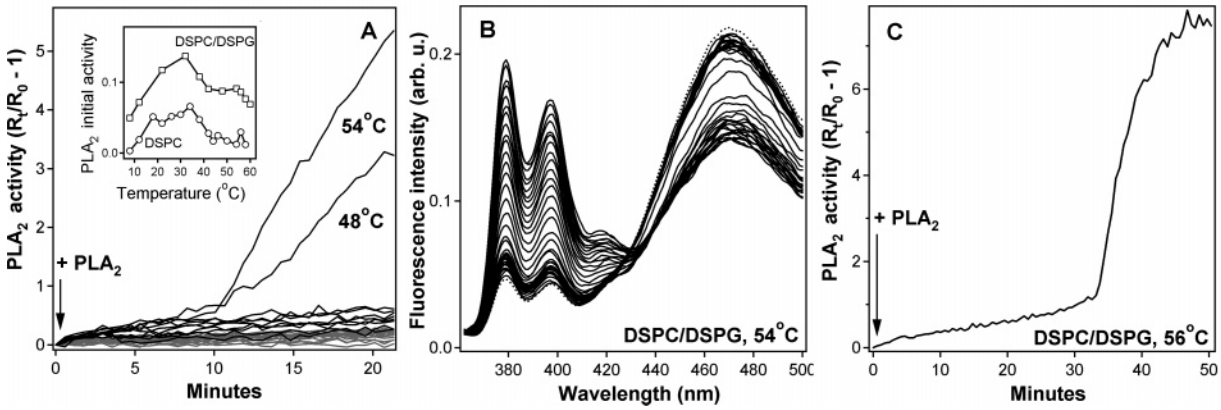

FIGURE 1: Temperature dependence of hIBPLA$_2$ activity against DSPC and DSPC/DSPG (7:3) vesicles. (A) Time course of lipid hydrolysis obtained by consecutively measuring fluorescence spectra of bisPyPC (2.5 mol % in membranes) with a periodicity of 1.7 min^{-1}. The dark and gray lines correspond to DSPC/DSPG and pure DSPC vesicles, respectively. PLA$_2$ was added between 0 and 0.5 min, followed by measurement of 36 spectra after addition of PLA$_2$. The inset shows the temperature dependencies of the initial rates of lipid hydrolysis (change in $R_t/R_0 - 1$ per minute) for both types of vesicles, as indicated. Panel B shows representative fluorescence spectra of bisPyPC in DSPC/DSPG membranes at 54 °C, where onset of high PLA$_2$ activity was detected at around 10 min after addition of PLA$_2$. The dotted line corresponds to vesicles before addition of PLA$_2$, after which 36 spectra were recorded that show an increase in the monomer signal (two peaks at lower wavelengths) and a decrease in the excimer signal (peak around 470 nm). The spectra have been smoothed using an 11-point Savitzky−Golay algorithm. Panel C shows the time dependence of lipid hydrolysis by PLA$_2$ for DSPC/DSPG vesicles at 56 °C, when the onset of high PLA$_2$ activity occurs ~34 min following addition of PLA$_2$. Total lipid and PLA$_2$ concentrations were 0.4 mM and 0.5 μM, respectively. The buffer was 50 mM NaCl, 2 mM CaCl$_2$, and 50 mM Hepes (pH 7.4).

i.e., an increase in the monomer signal and a decrease in the excimer signal as a result of lipid hydrolysis, control experiments were conducted in which the temperature dependence of bisPyPC fluorescence was studied without PLA$_2$. To distinguish the temperature effects per se from lipid phase transition effects, lipids were used that undergo phase transitions at distinctly different temperatures. These included POPC, DMPC, DPPC, and DSPC without or with 30 mol % of the respective PGs. Both the monomer and excimer signals of bisPyPC demonstrated drastic changes at the lipid phase transition, which are presented in Figure 2 of the Supporting Information for DMPC and DMPC/DMPG (7:3) (here and in the forthcoming text molar ratios are shown). The monomer fluorescence intensity increases with increasing temperature, peaks at T_m, and then decreases. At $T < T_m$, the intensity of the excimer signal is lower than that of the monomer signal, but sharply increases to higher levels at T_m and stays high at $T > T_m$ (Figure 2A,B of the Supporting Information). This results in a sharp decline in the difference of the monomer and excimer intensities at T_m (Figure 2C of the Supporting Information). It should be noted that the phase transition for DMPC/DMPG (7:3) occurs at 4−6 °C higher temperatures than for pure DMPC membranes. Similar trends were detected for POPC, DPPC, DSPC, and their combinations with 30% PGs with identical acyl chains. For DPPC and DPPC/DPPG membranes, the phase transition occurred at 40−43 °C and for DSPC and DSPC/PSPG membranes at 52−56 °C (not shown). For POPC membranes, phase transition has not been detected between 2 and 56 °C, as expected. For combinations of POPC with 30 or 50 mol % POPG, phase transitions were detected around 5 and 10 °C, respectively, as judged by the peak in the pyrene monomer signal (not shown). Higher transition temperatures of membranes containing increasing fractions of anionic lipid may result from Ca^{2+} binding to negatively charged membranes, an effect that is known to increase the thermal stability of lipid bilayers (*40*). In phase transition experiments shown in Figure 1 of the Supporting Information this effect is not detected because they have been conducted in the absence of Ca^{2+} (1 mM EGTA), while a buffer with 2 mM CaCl$_2$ was used in experiments presented in Figure 2 of the Supporting Information to replicate the conditions under which PLA$_2$ activity was measured.

Temperature Dependence of PLA$_2$ Activity. The temperature dependence of the activity of hIBPLA$_2$ against DSPC and DSPC/DSPG (7:3) LUVs was measured between 8 and 60 °C. When DSPC vesicles were equilibrated at a given temperature and then PLA$_2$ was added, little activity was recorded during 21 min (Figure 1A). With DSPC/DSPG (7:3) vesicles, again very low initial PLA$_2$ activity was detected, although the measured activities were nearly 2-fold higher than those with pure DSPC vesicles (Figure 1A, inset). In both cases, the initial catalytic rate of PLA$_2$ showed a maximum between 30 and 40 °C. Interestingly, for DSPC/DSPG vesicles onset of high PLA$_2$ activity occurred at 48 and 54 °C approximately 10 min following addition of PLA$_2$ to the vesicles (Figure 1A). Representative time-dependent fluorescence spectra of bisPyPC in DSPC/DSPG vesicles at 54 °C are shown in Figure 1B. Abrupt activation of PLA$_2$ after a relatively long lag time was detected with DSPC/DSPG at temperatures close to the phase transition temperature of these lipids (55 ± 0.5 °C), but not with pure DSPC vesicles. At 56 °C, PLA$_2$ activation against DSPC/DSPG vesicles was detected at ~34 min after addition of PLA$_2$ to the vesicles (Figure 1C). Notably, while the duration of the lag increases as the temperature increases from 48 to 56 °C, the activity that follows is significantly higher at higher temperatures.

At temperatures higher than 56 °C, the lag-burst effect (i.e., abrupt transition from a low to a high activity state) was not detected for at least 1 h of incubation of PLA$_2$ with DSPC/DSPG vesicles. Two lines of evidence suggest that this was not due to inactivation of PLA$_2$ at high temperatures. First, a very strong increase in PLA$_2$ activity occurred when PLA$_2$ was incubated with DSPC/DSPG vesicles at temper-

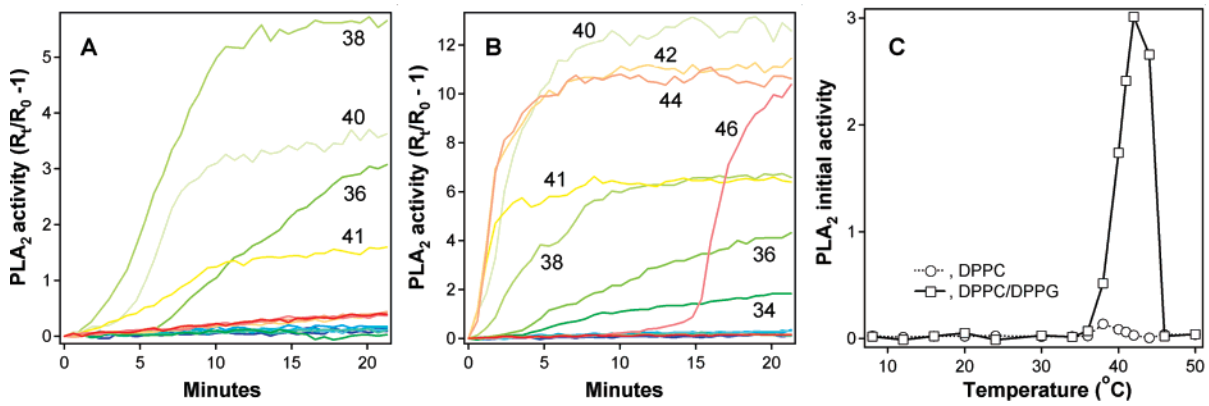

FIGURE 2: Temperature dependence of hIBPLA$_2$ activity against DPPC (A) and DPPC/DPPG (7:3) vesicles (B). Panels A and B show the kinetic curves of lipid hydrolysis, as measured by the change in the fluorescence spectra of bisPyPC in vesicle membranes (see the Materials and Methods). A change in color from blue to red corresponds to temperatures from 8 to 50 °C, and the curves are labeled with the corresponding temperatures wherever possible. The temperature dependencies of the initial rates of lipid hydrolysis for both types of membranes, i.e., the change in $R_t/R_0 - 1$ per minute, are shown in panel C. The experimental conditions are as in Figure 1.

atures well below T_m, e.g., 22−42 °C, and then the temperature was rapidly increased to 56−58 °C. One of these temperature shift experiments is demonstrated in Figure 3 of the Supporting Information. During incubation of hIBPLA$_2$ with DSPC/DSPG (7:3) vesicles at 32 °C for 21 min, the enzyme shows a low level of activity, values of ($R_t/R_0 - 1$) barely reaching 0.5 (Figure 3A,B of the Supporting Information). A temperature shift to 58 °C results in a sharp increase in PLA$_2$ activity, with ($R_t/R_0 - 1$) values exceeding 4.0. No abrupt increase in PLA$_2$ activity occurs when the enzyme is incubated with vesicles for a long time (up to 1 h) at either 32 or 58 °C (the latter is demonstrated in Figure 3C of the Supporting Information). Second, when PLA$_2$ is incubated with DSPC/DSPG vesicles at 58 °C for 30 min and then the temperature is shifted to 54 °C, onset of high activity occurs immediately (not shown). This latter result cannot be interpreted by a reversible inactivation of PLA$_2$ at ≥58 °C because the above data demonstrate high activity of PLA$_2$ at 58 °C following a temperature shift.

Although spontaneous lag-burst activation of PLA$_2$ was not observed with pure DSPC vesicles at any temperature, we did detect high activity of PLA$_2$ against these vesicles in temperature shift experiments. A strong increase in PLA$_2$ activity occurred when the temperature was rapidly changed from relatively low values to temperatures close to T_m, e.g., 56−58 °C. Small shifts in temperature, e.g., from 56 to 58 °C, did not cause PLA$_2$ activation, but when the temperature was lowered, e.g., to 42 °C, and then rapidly increased back to 58 °C, a very strong increase in PLA$_2$ activity was detected (see Figure 4 in the Supporting Information).

With zwitterionic DPPC vesicles, onset of significant PLA$_2$ activity occurs at temperatures close to T_m, e.g., 38−41 °C (Figure 2A). With anionic DPPC/DPPG membranes, the temperature range corresponding to high PLA$_2$ activity is wider, and both the rate and the degree (i.e., the values of $R_t/R_0 - 1$) of lipid hydrolysis are significantly higher compared to DPPC vesicles (Figure 2A,B). Between 38 and 44 °C, high PLA$_2$ activity was recorded immediately following addition of PLA$_2$ to DPPC/DPPG vesicles. At 34 and 36 °C, onset of relatively high activity occurs at 3−4 min, and at 46 °C a burst of high activity takes place at around 15 min. At temperatures farther away from T_m in both directions, e.g., at 30 or 50 °C, no onset of activity was detected for up to 45 min. When the initial PLA$_2$ activities are plotted against temperature, a sharp activity peak is detected around T_m of DPPC/DPPG membranes, whereas the increase in the initial PLA$_2$ activity around T_m is much weaker for DPPC membranes (Figure 2C).

As in the case of distearoyl lipids described above, a temperature shift from low or high temperatures, where little activity is measured, to temperatures close to T_m results in strong activation of PLA$_2$. This effect is demonstrated by two examples when a temperature shift from 8 to 41 °C in the presence of DPPC/DPPG vesicles causes immediate strong activation of PLA$_2$, and such a temperature shift with pure DPPC vesicles results in a high level of activity preceded by several minutes of relatively low activity (Figure 5 in the Supporting Information). Similar effects occur when the temperature is brought to 41 °C from higher levels, such as 50 °C (not shown). When the temperature is changed from "very low" values (e.g., 8 °C) to "very high" values (e.g., 50 °C), none of which support PLA$_2$ activity, again significant lipid hydrolysis is detected. However, this probably results from PLA$_2$ activation when the temperature passes through T_m (41−42 °C) and not by enzyme activation at 50 °C.

Similar to the results obtained on DSPC and DSPC/DSPG membranes, the enzyme activity that is reached upon a temperature shift to a value close to T_m strongly exceeds the activity measured after equilibration of PLA$_2$ at the same temperature without a temperature shift. For example, at 41 °C the values of $R_t/R_0 - 1$ reach approximately 1.6 for DPPC membranes (Figure 2A), while a value of ∼3 is reached following a temperature shift from 8 to 41 °C (Figure 5 in the Supporting Information).

The behavior of hIBPLA$_2$ in the presence of DMPC and DMPC/DMPG vesicles is similar to that with DPPC and DPPC/DPPG vesicles, with distinct quantitative differences. Again, initial high PLA$_2$ activity is detected at temperatures near T_m of these lipids, i.e., 22−28 °C (Figure 3). The maximum initial rate is reached around 23 °C for DMPC and around 28 °C for DMPC/DMPG membranes. This is similar to a slightly higher temperature optimum for PLA$_2$ activity against DPPC/DPPG compared to pure DPPC membranes (Figure 2) and is consistent with a ∼5 °C higher

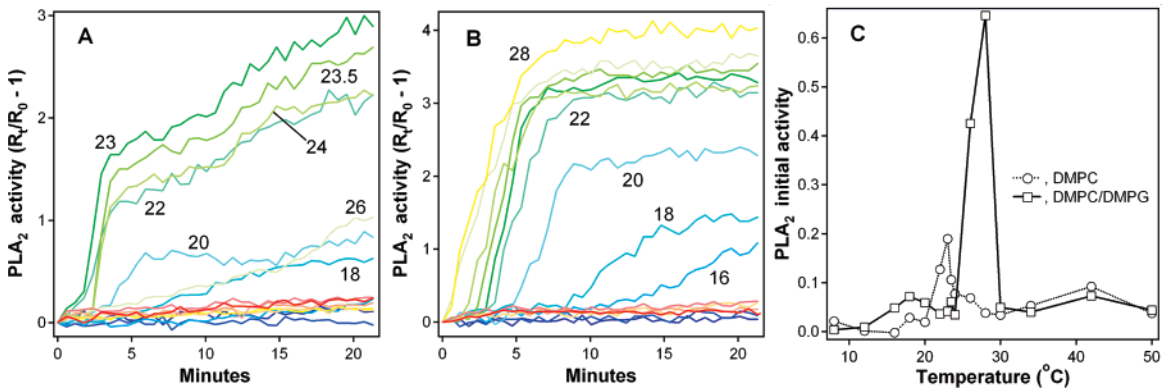

FIGURE 3: Temperature dependence of hIBPLA$_2$ activity against DMPC (A) and DMPC/DMPG (7:3) vesicles (B). Panels A and B show the kinetics of lipid hydrolysis, as measured by the change in the fluorescence spectra of bisPyPC in vesicles. A change in color from blue to red corresponds to temperatures from 8 to 50 °C, and curves that show significant PLA$_2$ activity are labeled with the respective temperatures. The same color code is used in panels A and B. The temperature dependencies of the initial rates of lipid hydrolysis for both types of membranes, i.e., the change in $R_t/R_0 - 1$ per minute, are shown in panel C. The experimental conditions are as in Figure 1.

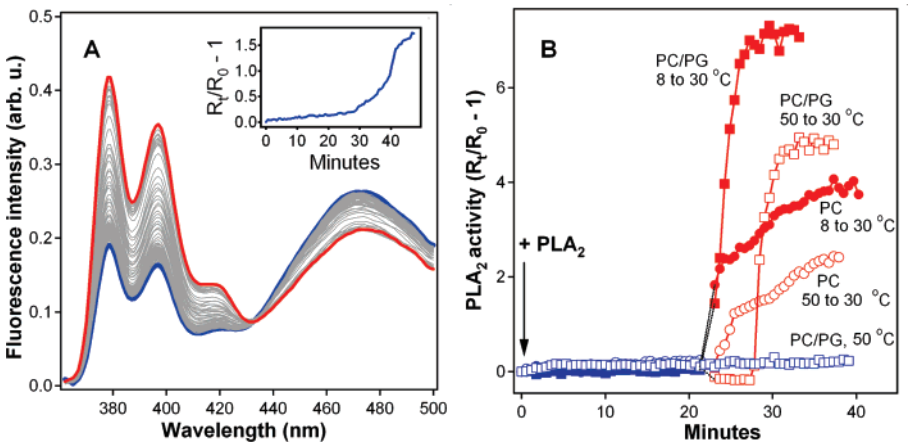

FIGURE 4: Spontaneous or temperature-induced activation of hIBPLA$_2$ on DMPC or DMPC/DMPG membranes. Panel A shows the spectra of bisPyPC in DMPC vesicles at 28 °C before (blue line) and after addition of PLA$_2$. The red line is the last (number 80) spectrum measured after addition of PLA$_2$. The inset is PLA$_2$ activity ($R_t/R_0 - 1$; see the Materials and Methods) plotted versus time. PLA$_2$ was added between 0 and 0.5 min. Panel B shows induction of high PLA$_2$ activity by a temperature shift in the presence of DMPC or DMPC/DMPG vesicles. Initially the vesicles were incubated at 8 or 50 °C, PLA$_2$ was added between 0 and 0.5 min, and activities were measured by recording the spectra of bisPyPC (2.5 mol % in vesicles). Squares and circles correspond to DMPC/DPMG and pure DMPC vesicles, respectively. Data obtained before the temperature shift are presented by blue symbols and those after the temperature shift by red symbols. One control experiment is presented (open blue squares), which shows absence of PLA$_2$ activation on DMPC/DMPG vesicles at 50 °C for up to 40 min. The experimental conditions are as in Figure 1.

phase transition temperature of DMPC/DMPG versus pure DMPC membranes in the presence of 2 mM Ca^{2+} (Figure 2B,C of the Supporting Information). The temperature dependence of interfacial activation of PLA$_2$ can be clearly seen from data obtained on DMPC/DMPG membranes. Below 16 °C, no activation occurs during the first 21 min of incubation of PLA$_2$ with vesicles, whereas between 16 and 28 °C onset of increasingly high PLA$_2$ activity is detected that is preceded by a lag phase, the duration of which decreases with increasing temperature (Figure 3B). It is noteworthy that the maximum initial rate of lipid hydrolysis in the presence of anionic DMPC/DMPG or DSPC/DSPG membranes exceeds that with the corresponding zwitterionic lipids (DMPC and DSPC, respectively) by approximately 2−3-fold (Figures 1 and 3), whereas such a difference between DPPC/DPPG and DPPC membranes is more than 20-fold (Figure 2). An explanation of this effect is presented in the Discussion.

The data from Figure 3A,B show that higher initial PLA$_2$ activities result in shorter lag times that are followed by higher rates of lipid hydrolysis at the "burst". In many of those cases when onset of high activity is not detected at a given temperature during the first 21 min, PLA$_2$ activation can be induced either spontaneously at later times or by a temperature shift from higher or lower values to a given temperature. Spontaneous activation of PLA$_2$ occurs at temperatures that are not too low or too high compared to the T_m. For example, hIBPLA$_2$ shows low activity against DMPC vesicles at 28 °C for about 25 min, which is followed by a gradual and then sharper increase in activity (Figure 4A). In the case of DMPC/DMPG membranes, little activity is measured at 30 °C for up to 40 min following addition of PLA$_2$. However, when PLA$_2$ is incubated for ~20 min with the vesicles at lower or higher temperatures (i.e., 8 or 50 °C when PLA$_2$ shows no or little activity for at least 40 min) and then the temperature is shifted to 30 °C, very high PLA$_2$ activities are recorded either immediately or following several minutes of delay (Figure 4B).

The activity of hIBPLA$_2$ against POPC and POPC/POPG membranes was very low within the temperature range from 2 to 56 °C. Representative data on the time dependence of lipid hydrolysis at 20, 36, and 56 °C are shown in Figure 5.

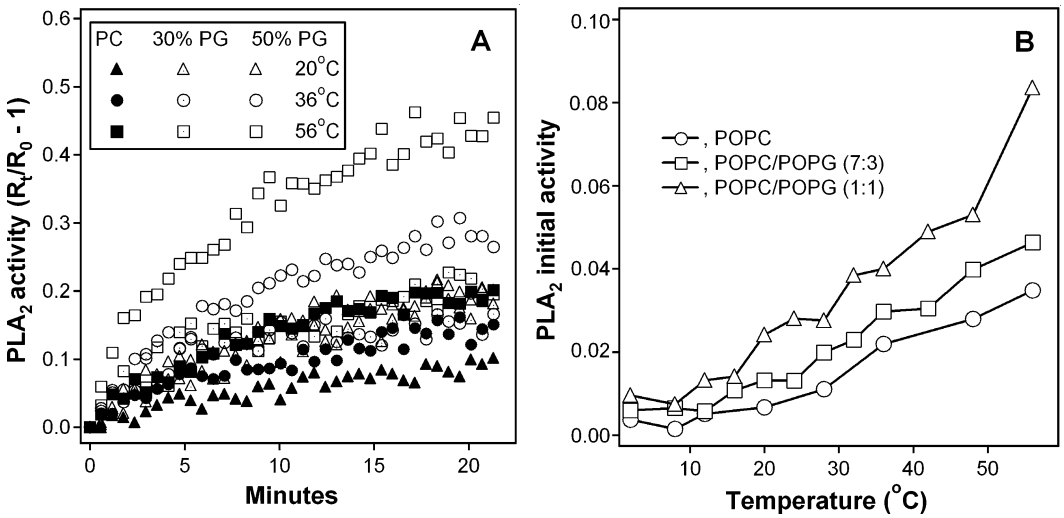

FIGURE 5: Temperature dependence of hIBPLA$_2$ activity against POPC and POPC/POPG vesicles. Panel A shows the kinetic curves of lipid hydrolysis with membranes containing 0, 30, and 50 mol % POPG at 20, 36, and 56 °C, as indicated. The temperature dependencies of the initial rates of lipid hydrolysis for both types of membranes, i.e., the change in $R_t/R_0 - 1$ per minute, are shown in panel B. The experimental conditions are as in Figure 1.

Although an increase in POPG content to 50 mol % resulted in better PLA$_2$ activities, these levels were still 10-fold (or more) lower than activities that could be measured with the other lipids described above. In no case was spontaneous onset of high PLA$_2$ activity observed, even when PLA$_2$ was incubated with POPC/POPG (1:1) vesicles for up to 1 h at various temperatures. One peculiarity of the POPC/POPG system compared to the lipids with saturated acyl chains is that the T_m of POPC and POPG lies in the freezing (or at least near-freezing) temperature region. It was not possible to induce high PLA$_2$ activity by a temperature shift from relatively high values to those close to T_m (e.g., from 42 to 1 °C, from 28 to 1 °C, and from 20 to 2 °C). Temperature shifts from low to high values (e.g., from 2 to 20 °C or from 8 to 40 °C) were equally ineffective. In several experiments the POPC/POPG (1:1) sample in the presence of hIBPLA$_2$ was rapidly frozen below 0 °C for ~10 min and then returned to the initial temperature (42, 20, or 8 °C). In these experiments, the lipid hydrolysis after the return to the initial temperature was slightly higher than it would be if left at that temperature without thermal alterations. One such example is shown in Figure 6 of the Supporting Information (compare the slopes before and after the shift to −3 °C). Although this is qualitatively reminiscent of PLA$_2$ activation at T_m (e.g., Figure 5 in the Supporting Information), the magnitude of the putative PLA$_2$ activation after freezing and thawing is too small to be considered significant.

Membrane Insertion of hIBPLA$_2$. The onset of high PLA$_2$ activity could be induced by various factors, including deeper insertion into the membrane. To clarify whether activation of PLA$_2$ at T_m of the lipid involves a component of deeper membrane insertion, we have conducted quantitative analysis of insertion of hIBPLA$_2$ into DMPC/DMPG membranes as a function of temperature. The method of quenching the fluorescence of the single Trp[3] of hIBPLA$_2$ by brominated lipids has been used, as described previously (*27*). It was important to first determine how Br$_2$PCs affect the lipid phase transition, which was measured using the temperature dependence of laurdan fluorescence, as in Figure 1 of the Supporting Information. The presence of 20 mol % Br$_2$PCs in DMPC/DMPG membranes resulted in almost complete linearization of the temperature-dependent change in laurdan GP (not shown). With 10 mol % Br$_2$PCs, the thermal profile of laurdan GP maintained both the sigmoidal shape and the value of T_m, although the phase transition was less cooperative compared to that for membranes without brominated lipids (Figure 7 of the Supporting Information). Because 10 mol % Br$_2$PCs did not eradicate the lipid phase transition and still could cause significant quenching of PLA$_2$ fluorescence (see below), this content of brominated lipids was used in membrane insertion experiments. Since in these experiments a relatively high PLA$_2$ concentration was used, the effect of PLA$_2$ on the lipid phase transition was also assessed. LUVs were made that contained DMPC, DMPG, 6,7-Br$_2$PC, and laurdan at molar ratios of 59:30:10:1, and fluorescence spectra were measured between 4 and 50 °C in the presence of 6 μM hIBPLA$_2$. Laurdan could be excited either directly, using $\lambda_{exc} = 360$ nm, or through excitation of the tryptophans of hIBPLA$_2$ and resonance energy transfer (RET) from tryptophans to laurdan, both of which generated good laurdan fluorescence spectra (Figure 6A,B). Note that laurdan cannot be excited below 300 nm (*29*), indicating that laurdan excitation in Figure 6A results completely from RET. In Figure 6A the Trp fluorescence of hIBPLA$_2$ can be clearly seen, although its intensity is not high because of quenching by both laurdan and 6,7-Br$_2$PC. The important finding here is that the combination of both brominated lipid and membrane-bound PLA$_2$ does not strongly affect the phase transition of DMPC/DMPG membranes (Figure 6C), indicating that the dependence of membrane insertion of PLA$_2$ on the lipid phase transition can be measured under these conditions.

To quantitatively determine the depth of membrane insertion of PLA$_2$ at different temperatures, differential quenching of Trp fluorescence of PLA$_2$ by Br$_2$PCs has been measured as a function of temperature. Representative temperature-dependent spectra in the presence of DMPC/DMPG vesicles and those containing 10 mol % 9,10-Br$_2$PC are shown in Figure 8 of the Supporting Information. Temperature dependencies of Trp fluorescence intensities at 325 nm are shown in Figure 7A for hIBPLA$_2$ free in buffer, as well as bound to DMPC/DMPG vesicles without and with

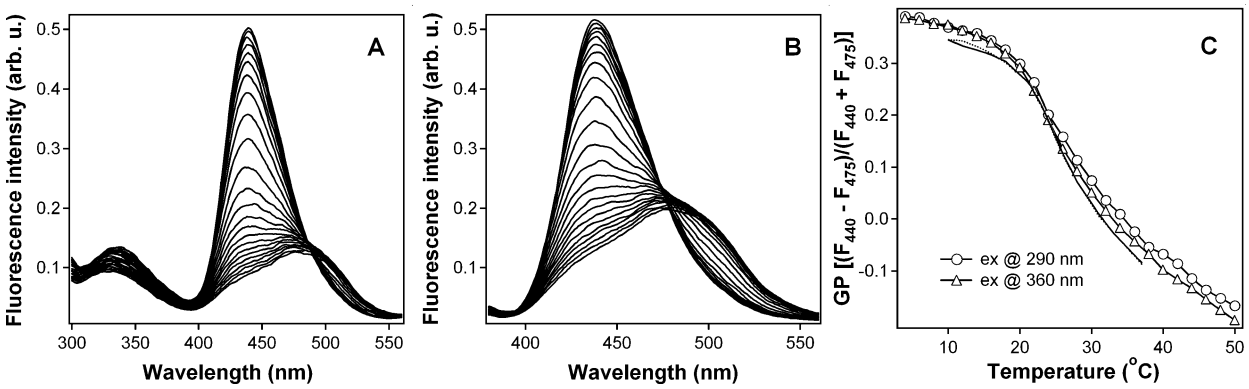

FIGURE 6: Phase transition of DMPC/DMPG membranes containing 1 mol % laurdan and 10 mol % 6,7-Br_2PC in the presence of 6 μM hIBPLA_2. The fraction of DMPG is 30 mol %. In panels A and B, excitation at 290 or 360 nm was used, respectively. The temperature increases from 4 to 50 °C in 2 °C steps, which corresponds to decreasing intensities at 440 nm. Panel C shows the temperature dependence of laurdan GP at two different excitations, as indicated. Gray solid and dotted lines show the phase transition of DMPC/DMPG (7:3) vesicles (heating and cooling, respectively) in the absence of Br_2PC and PLA_2 for comparison. The buffer was 50 mM NaCl, 1 mM EGTA, and 50 mM Hepes (pH 7.4).

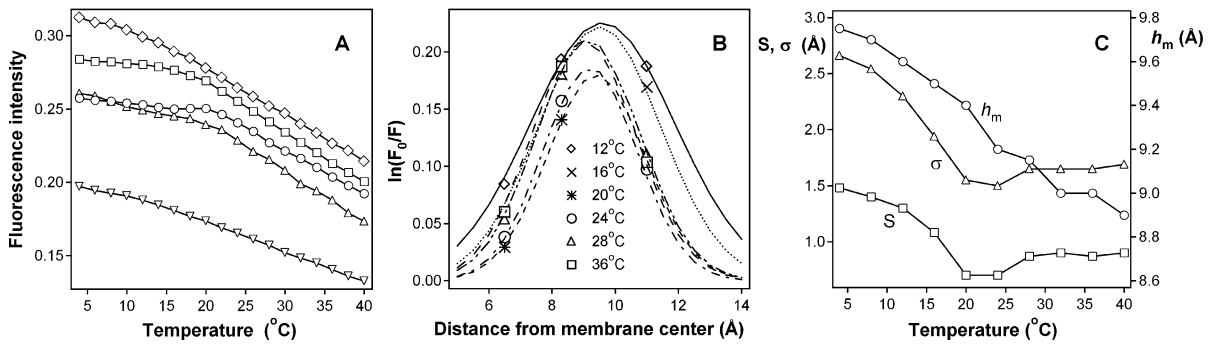

FIGURE 7: (A) Temperature dependence of tryptophan fluorescence emission intensities of 6 μM hIBPLA_2 free in the buffer (inverse triangles) and with DMPC/DMPG vesicles without (rhombuses) or with 10 mol % 6,7-Br_2PC (circles), 9,10-Br_2PC (triangles), or 11,12-Br_2PC (squares). The content of DMPG is 30 mol %, and the sum of DMPC and Br_2PC is 70 mol %. The total lipid concentration and the buffer are the same as in Figure 6. (B) Dependence of tryptophan fluorescence quenching by Br_2PCs on the locations of bromines with respect to the membrane center for selected temperatures, as indicated. (C) Temperature dependence of the distance from the membrane center (h_m), dispersion (σ), and the area under the distribution curve (S) that describe insertion of hIBPLA_2 into DMPC/DMPG membranes.

each of the three quenchers, i.e., 6,7-, 9,10-, and 11,12-Br_2-PC. Similar plots were obtained at other fixed wavelengths, but this particular wavelength was chosen for further analysis because (a) it has been recommended on the basis of previous work on membrane-bound proteins (*41*) and (b) the blue shift of Trp fluorescence upon membrane binding of hIBPLA_2 (*27*, *28*) implies that the signal at $\lambda < \lambda_{max}$ reflects the properties of membrane-bound protein better than the signal at $\lambda \geq \lambda_{max}$. The data of Figure 7A show that (a) in all cases the Trp emission intensity decreases with increasing temperature and (b) Br_2PCs quench Trp fluorescence of PLA_2 to different degrees. The overall fluorescence intensity is determined by $\phi_F = k_F/\{k_F + k_{ic} + k_{is} + k_q[Q]\}$, where ϕ_F is the fraction of excited fluorophores that emit fluorescence with a rate constant of k_F, while k_{ic}, k_{is}, and k_q are the rate constants of internal conversion, intersystem crossing, and direct quenching by a quencher at concentration [Q] (*42*). (A more detailed discussion can be found in ref *42*, pp 436−439.) The main reasons for a decrease in protein fluorescence intensity with rising temperature are believed to be an increase in k_{ic} and more efficient collisional quenching by water or dissolved oxygen at higher temperatures (*42*). The fact that Trp emission of membrane-bound PLA_2 is lower when Br_2PCs are present in the membrane indicates differential quenching of Trp by Br_2PCs. At low temperatures the quenching efficiency changes in the sequence 6,7-Br_2-PC > 9,10-Br_2PC > 11,12-Br_2PC, while at higher temperatures the sequence is 9,10-Br_2PC > 6,7-Br_2PC > 11,12-Br_2PC. A straightforward interpretation of these data is that for solid-state membranes PLA_2 binds to the membrane surface peripherally so its Trp^3 is quenched stronger by bromines of 6,7-Br_2PC located closer to the lipid−water interface while for the fluid membranes PLA_2 moves deeper into the hydrocarbon region of the membrane closer to the 9,10-positions of the lipid acyl chains. This was verified quantitatively by calculating the quenching efficiencies at each temperature, plotting them against the distance of bromines from the membrane center (*34*), and fitting those plots with the distribution curves presented by eq 1. The three parameters that describe fluorescence quenching at each temperature (S, σ, and h_m) were deduced from best fits between the simulated distribution curves and experimental data. Given the bell shape of the curves, only one unique combination of these three parameters can properly describe the data, implying reliability of the parameters. Experimental data for selected temperatures, along with simulated curves, are presented in Figure 7B, and temperature dependencies of the quenching parameters are shown in Figure 7C. The parameters S and σ decrease with increasing temperature at $T < T_m$ and then experience little change above T_m. A decrease of the overall efficiency of quenching can be explained by easier dissociation between the fluorophore and

the quencher because of higher lateral diffusion of both PLA_2 and Br_2PCs at higher temperatures (*36*). The fact that this occurs at $T < T_m$ probably reflects the steep heat-induced decrease in the microviscosity of phospholipid membranes below but not above T_m (*43*). The location of Trp^3 of $hIBPLA_2$ with respect to the membrane center is ~9.8 Å at 4 °C and gradually changes to 8.9 Å upon an increase of temperature to 40 °C. Thus, the change in temperature from 4 to 40 °C causes a very modest change in the membrane insertion depth of PLA_2, indicating that PLA_2 inserts into the membrane only ~1 Å deeper upon the transition of the membrane from the gel to the liquid-crystalline phase.

DISCUSSION

Although the effects of temperature and the lipid phase transition on PLA_2 activation have been studied previously (see the introduction), the use of different lipids and experimental conditions makes it difficult to reconcile the contradictory results. Activation of PLA_2 after the lag phase is thought to result from accumulation of a critical fraction of reaction products (free fatty acid and lysophospholipid) in the membrane. Apitz-Castro et al. (*8*) found that accumulation of a total of ~5 mol % (or ~9 mol % in the outer layer) reaction products caused activation of $pIBPLA_2$ against sonicated DMPC vesicles at 17 °C, but up to $X_p = 20$ mol % of both reaction products had to be added externally to eliminate the lag. In the case of DPPC LUVs at 38 °C, $X_p = 6.9-8.3$ mol % reaction products abolished the lag (*11*), and for supported planar POPC membranes at 25 °C the lag phase terminated when $5 \pm 3\%$ of the lipid was hydrolyzed (*15*). Henshaw et al. (*14*) have shown that the effects of the reaction products are not simple and depend on factors such as pH, Ca^{2+} concentration, and temperature. Our data support this notion and indicate that PLA_2 cannot be activated just because a certain fraction of the lipid has been hydrolyzed. The effect of the reaction products on the onset of high PLA_2 activity is determined by the temperature-dependent physical state of the membrane. Thus, at 48−54 °C PLA_2 activity against DSPC/DSPG (7:3) vesicles is triggered when ~8% of the lipid is hydrolyzed, but at 56 °C PLA_2 activation occurs at ~15% lipid hydrolysis (Figure 1). Higher values of X_p above T_m are in accord with the data of Henshaw et al. (*14*) obtained on DPPC LUVs in the presence of 1 mM Ca^{2+}. At lower temperatures PLA_2 activation does not occur when the fraction of hydrolyzed lipid exceeds 8% (Figure 1). As shown in Figure 3 of the Supporting Information, at 32 °C hydrolysis of ~13% of the lipid in DSPC/DSPG (7:3) membranes fails to activate PLA_2, but a temperature shift to 58 °C immediately results in high enzyme activity. On the other hand, our data present many examples when a temperature shift causes strong PLA_2 activation even in the absence of any considerable prior lipid hydrolysis (Figure 4 here and Figure 5 of the Supporting Information).

While Apitz-Castro et al. (*8*) interpret the effect of reaction products on PLA_2 activity by increased membrane binding affinity of PLA_2, product-induced lateral phase separation and membrane structural perturbations have also been implicated (*11*−*14*, *44*). Henshaw et al. (*14*) explained the higher values of X_p above T_m in terms of sequestration of the membrane-bound PLA_2 by the product at high temperatures. Our data suggest that the major temperature-dependent factor that facilitates PLA_2 activation is the structural perturbation of the membrane. When PLA_2 is added to vesicles that are equilibrated at a given temperature (e.g., at 30 °C for DMPC/DMPG membranes), little activity is recorded (Figure 3B), but thermal perturbation of the membrane by a rapid shift of temperature to 30 °C from low or high temperatures in the presence of PLA_2 results in very high PLA_2 activities (Figure 4B). Qualitatively similar data are obtained also for membranes composed of other lipids (e.g., Figure 4 in the Supporting Information). These results lead to a conclusion that structural heterogeneities in the membrane, such as irregular boundaries between regularly packed lipid domains, probably facilitate PLA_2 binding and subsequent activation. This accords with an earlier finding of PLA_2 activation by adding vesicles with high curvature and hence with a high degree of packing defects (*13*). According to this logic, the increased lateral mobility of reaction products at $T > T_m$ apposes domain formation, and therefore, larger fractions of products are required to compensate this effect and activate PLA_2.

The above mechanism in conjunction with our temperature shift experiments sheds light on previously observed thermal effects in PLA_2 activation. For example, Menashe et al. (*17*) explained PLA_2 activation upon a shift of temperature from $T < T_m$ to $T \geq T_m$ by stronger membrane binding of PLA_2 at lower temperatures. If this were the case, PLA_2 would not be activated upon a temperature shift to $\sim T_m$ from higher temperatures. Our data show that this indeed happens (Figure 4), indicating that thermal perturbations and not stronger membrane binding of PLA_2 at $T < T_m$ cause PLA_2 activation. The only requirement is that the final temperature should not be too far from T_m.

Thermal effects in PLA_2 depend on the thermotropic phase transition of the lipid at T_m and the intrinsic optimal temperature for PLA_2 activity, T_{opt}. The highest PLA_2 activities are reached when these two temperatures are close to each other. Because the value of T_{opt} appears to be between 30 and 40 °C, which is close to T_m for DPPC and DPPG, and because PLA_2 activity increases with the anionic surface charge of the membrane, the highest activity of $hIBPLA_2$ is recorded around the phase transition of DPPC/DPPG (7:3) membranes (Figure 2). PLA_2 activity decreases with increasing difference between T_m and T_{opt}. For example, PLA_2 activity with POPC or POPC/POPG membranes is very low, with no onset of high activity under any conditions (Figure 5 here and Figure 6 in the Supporting Information) because T_m is very low compared to T_{opt}. At temperatures close to T_{opt} (30−40 °C) the enzyme activity is low because PLA_2 is only able to be highly active around T_m. On the other hand, at temperatures close to T_m of these lipids (e.g., 2−10 °C) PLA_2 shows low activity because it is too far from its intrinsically optimal temperature. In other words, because of the dependence of PLA_2 activity on T_{opt}, the enzyme may not show any significant activity even at T_m when T_m is too far from T_{opt}.

It should also be noted that the immediate microenvironment of membrane-bound PLA_2 may be different from the bulk membrane properties, which may impede accurate determination of the actual dependence of PLA_2 activity on the temperature-dependent state of the membrane. This effect

may not be detected at low PLA_2:lipid ratios, but should manifest itself at higher PLA_2 concentrations corresponding to large surface occupancies of bound PLA_2. Figure 6 shows the effect of PLA_2 on the phase transition of DMPC/DMPG (7:3) membranes under conditions when ~80% of PLA_2 is membrane-bound (see the Materials and Methods, Membrane Insertion of PLA_2). Taking into account the total lipid and PLA_2 concentrations (800 and 6 μM, respectively) and a binding stoichiometry of PLA_2:lipid $\approx$ 1:36 (*28*, *33*), it appears that nearly 22% of the total lipid is PLA_2-bound, and yet there is little disturbance of the lipid phase transition. In activity experiments, 0.5 μM PLA_2 has been used, corresponding to a much smaller membrane surface occupancy by PLA_2. These considerations show that under our experimental conditions PLA_2 binding does not significantly perturb the membrane thermal properties.

Despite the complex dependence of PLA_2 activity on various factors, such as the membrane charge, T_m, and T_{opt}, it is possible to model the temperature dependence of PLA_2 activity by using relatively simple analytic formulations. This can be done, for example, by combination of two normal distribution functions that account for maximal activities around T_m and T_{opt}. The width and the height of each peak can be adjusted by corresponding dispersions, δ_1 and δ_2. The dependence of the overall activity on the membrane charge can be provided through a preexponential coefficient, A_{max}, and the dependence on the difference between T_m and T_{opt} by a term involving $|T_m - T_{opt}|$:

$$A = \frac{A_{max}}{1 + |T_m - T_{opt}|}\left\{\frac{1}{\delta_1}\exp\left[-\frac{(T - T_m)^2}{2\delta_1^{\,2}}\right] + \frac{1}{\delta_2}\exp\left[-\frac{(T - T_{opt})^2}{2\delta_2^{\,2}}\right]\right\} \quad (2)$$

As shown in Figure 9 of the Supporting Information, this relationship describes the temperature dependence of PLA_2 activity quite reasonably. When T_m and T_{opt} are the same (e.g., 40 °C), a high activity peak occurs at that temperature, as in the case of DPPC/DPPG membranes (Figure 2C, squares). When T_{opt} is left unchanged but T_m is changed to 24 °C, a sharp peak at T_m and a second wider and weaker peak at T_{opt} occur, as in the case of DMPC/DMPG membranes (Figure 3C, squares). Note that the activity peak in Figure 9A of the Supporting Information is much stronger than that at T_m in panel B. This is the result of $T_m = T_{opt}$ in panel A but not in panel B, which reasonably models the real situation of a substantially higher PLA_2 activity peak with DPPC/DPPG than with DMPC/DMPG or DSPC/DSPG membranes (see Figures 1−3). Note that in Figure 9 of the Supporting Information a value of $A_{max} = 1$ has been used; the levels of activity at various membrane charge densities can be adjusted by choosing appropriate values of A_{max}.

There has been considerable controversy regarding the relationship between activation of secreted PLA_2's and membrane insertion. While several groups have suggested that the onset of high activity may result from deeper insertion of PLA_2 into the membrane (*9*, *15*, *21*, *23*), others have rejected the possibility of any significant membrane insertion of these enzymes (*8*, *25*). We have shown previously that hIBPLA$_2$ inserts into POPC/POPG membranes so the Trp^3 reaches a depth of ~9 Å from the membrane center (*26*, *27*), and here we are asking the question of whether membrane insertion changes significantly at T_m. As shown in Figure 7, the overall efficiency of quenching, S, decreases with increasing temperature at $T < T_m$ and then experiences small change above T_m. According to the static quenching mechanism, a decrease in quenching efficiency can be explained by easier dissociation between the fluorophore and the quencher because of higher lateral diffusion of both PLA_2 and Br_2PCs in more fluid membranes (*36*). The dispersion, σ, exhibits a similar behavior, indicating a sharper distance distribution as the temperature approaches T_m. Most importantly, the distance of Trp^3 of PLA_2 from the membrane center (h_m) decreases from 9.8 to 8.9 Å, i.e., undergoes a diminutive change when the temperature increases from 4 to 40 °C. This indicates that PLA_2 has one optimal mode of binding to a given membrane that does not change significantly in terms of membrane insertion during the lipid phase transition. Conceptually, this agrees with our earlier findings that hIBPLA$_2$ binds to phospholipid membranes in a way to optimally satisfy Coulombic, H-bonding, and hydrophobic interactions (*26*). Our model indicates that Lys^{121} and Lys^{122} of the membrane-bound enzyme are involved in ionic interactions with lipid phosphate groups, Arg^6, Lys^7, Lys^{10}, and Lys^{116} are H-bonded to the lipid carbonyl oxygens, and the side chains of Trp^3, Phe^{19}, and Leu^{20} are embedded in the membrane hydrocarbon region (*26*). Transition of the membrane from the gel to the liquid-crystalline phase would promote membrane insertion of the protein, but the ionic and H-bonding interaction at the level of the lipid polar groups would resist such insertion. Our present data indeed support this scenario.

In conclusion, while earlier studies suggested the existence of two membrane binding modes of PLA_2 and transition between these states upon activation (*5*, *23*, *24*), our data indicate that at least for hIBPLA$_2$ the difference between these two modes is not the depth of membrane insertion. This does not preclude the possibility that for PLA_2 isoforms for which nonpolar interactions play a greater role in membrane binding than electrostatic interactions, such as human group X PLA_2, deeper membrane insertion may be an important component of activation. This can only be clarified by further studies. Also, changes in other aspects that determine the membrane binding mode of PLA_2, such as the angular orientation, may contribute to the enzyme activation. In fact, our unpublished data obtained by polarized infrared spectroscopy show that the orientational order parameter of hIBPLA$_2$ undergoes a significant change upon transition from latency to the active state of the membrane-bound enzyme (Pande, A. H., and Tatulian S. A., unpublished data). These studies will be continued to reach a better understanding of the molecular mechanisms of activation of PLA_2's and other interfacial enzymes.

ACKNOWLEDGMENT

We thank Dr. Kathleen N. Nemec for her help in some experiments.

SUPPORTING INFORMATION AVAILABLE

Figures describing the lipid phase transition, PLA_2 activation upon temperature shift, fluorescence spectra of PLA_2

without and with 9,10-Br_2PC in membranes, and simulated curves modeling the temperature dependence of PLA_2. This material is available free of charge via the Internet at http://pubs.acs.org

REFERENCES

1. Six, D. A., and Dennis, E. A. (2000) The expanding superfamily of phospholipase A_2 enzymes: classification and characterization, *Biochim. Biophys. Acta 1488*, 1−19.
2. Nevalainen, T. J., Eerola, L. I., Rintala, E., Laine, V. J., Lambeau, G., and Gelb, M. H. (2005) Time-resolved fluoroimmunoassays of the complete set of secreted phospholipases A_2 in human serum, *Biochim. Biophys. Acta 1733*, 210−223.
3. Boilard, E., Rouault, M., Surrel, F., Le Calvez, C., Bezzine, S., Singer, A., Gelb, M. H., and Lambeau, G. (2006) Secreted phospholipase A_2 inhibitors are also potent blockers of binding to the M-type receptor, *Biochemistry 45*, 13203−13218.
4. Gelb, M. H., Min, J.-H., and Jain, M. K. (2000) Do membrane-bound enzymes access their substrates from the membrane or aqueous phase: interfacial versus non-interfacial enzymes, *Biochim. Biophys. Acta 1488*, 20−27.
5. Gadd, M. E., and Biltonen, R. L. (2000) Characterization of the interaction of phospholipase A_2 with phosphatidylcholine-phosphatidylglycerol mixed lipids, *Biochemistry 39*, 9623−9631.
6. Bezzine, S., Bollinger, J. G., Singer, A. G., Veatch, S. L., Keller, S. L., and Gelb, M. H. (2002) On the binding preference of human groups IIA and X phospholipase A_2 for membranes with anionic phospholipids, *J. Biol. Chem. 277*, 48523−48534.
7. Diraviyam, K., and Murray, D. (2006) Computational analysis of the membrane association of group IIA phospholipase A_2: A differential role for electrostatics, *Biochemistry 45*, 2584−2598.
8. Apitz-Castro, R., Jain, M. K., and de Haas, G. H. (1982) Origin of the latency phase during the action of phospholipase A_2 on unmodified phosphatidylcholine vesicles, *Biochim. Biophys. Acta 688*, 349−356.
9. Kinkaid, A., and Wilton, D. C. (1991) Comparison of the catalytic properties of phospholipase A_2 from pancreas and venom using a continuous fluorescence displacement assay, *Biochem. J. 278*, 843−848.
10. Burack, W. R., and Biltonen, R. L. (1994) Lipid bilayer heterogeneities and modulation of phospholipase A_2 activity, *Chem. Phys. Lipids 73*, 209−222.
11. Burack, W. R., Yua, Q., and Biltonen, R. L. (1993) Role of lateral phase separation in the modulation of phospholipase A_2 activity, *Biochemistry 32*, 583−589.
12. Burack, W. R., Dibble, A. R. G., Allietta, M. M., and Biltonen, R. L. (1997) Changes in vesicle morphology induced by lateral phase separation modulate phospholipase A_2 activity, *Biochemistry 36*, 10551−10557.
13. Lichtenberg, D., Romero, G., Menashe, M., and Biltonen, R. L. (1986) Hydrolysis of dipalmitoylphosphatidylcholine large unilamellar vesicles by porcine pancreatic phospholipase A_2, *J. Biol. Chem. 261*, 5334−5340.
14. Henshaw, J. B., Olsen, C. A., Farnbach, A. R., Nielson, K. H., and Bell, J. D. (1998) Definition of the specific roles of lysolecithin and palmitic acid in altering the susceptibility of dipalmitoylphosphatidylcholine bilayers to phospholipase A_2, *Biochemistry 37*, 10709−10721.
15. Wacklin, H. P., Tiberg, F., Fragneto, G., and Thomas, R. K. (2007) Distribution of reaction products in phospholipase A_2 hydrolysis, *Biochim. Biophys. Acta 1768*, 1036−1049.
16. Jain, M. K., Egmond, M. R., Verheij, H. M., Apitz-Castro, R., Dijkman, R., and de Haas, G. H. (1982) Interaction of phospholipase A_2 and phospholipid bilayers, *Biochim. Biophys. Acta 688*, 341−348.
17. Menashe, M., Romero, G., Biltonen, R. L., and Lichtenber, D. (1986) Hydrolysis of dipalmitoylphosphatidylcholine small unilamellar vesicles by porcine pancreatic phospholipase A_2, *J. Biol. Chem. 261*, 5328−5333.
18. Bell, J. D., and Biltone, R. L. (1989) Thermodynamic and kinetic studies of the interaction of vesicular dipalmitoylphosphatidylcholine with *Agkistrodon piscivorus piscivorus* phospholipase A_2, *J. Biol. Chem. 264*, 225−230.
19. Bell, J. D., Burnside, M., Owen, J. A., Royall, M. L., and Baker, M. L. (1996) Relationship between bilayer structure and phospholipase A_2 activity: interactions among temperature, diacylglycerol, lysolecithin, palmitic acid, and dipalmitoylphosphatidylcholine, *Biochemistry 35*, 4945−4955.
20. Sanchez, S. A., Bagatolli, L. A., Gratton, E., and Hazlett, T. L. (2002) A two-photon view of an enzyme at work: *Crotalus atrox* venom PLA_2 interaction with single-lipid and mixed-lipid giant unilamellar vesicles, *Biophys. J. 82*, 2232−2243.
21. Volwerk, J. J., Jost, P. C., de Haas, G. H., and Griffith, O. H. (1986) Activation of porcine pancreatic phospholipase A_2 by the presence of negative charges at the lipid-water interface, *Biochemistry 25*, 1726−1733.
22. Van der Wiele, F. C., Atsma, W., Roelofsen, B., van Linde, M., Van Binsbergen, J., Radvanyi, F., Raykova, D., Slotboom, A. J., and de Haas, G. H. (1988) Site-specific ϵ-NH_2 monoacylation of pancreatic phospholipase A_2. 2. Transformation of soluble phospholipase A_2 into a highly penetrating "membrane-bound" form, *Biochemistry 27*, 1688−1694.
23. Zhou, F., and Schulten, K. (1996) Molecular dynamics study of phospholipase A_2 on a membrane surface, *Proteins 25*, 12−27.
24. Burack, W. R., Gadd, M. E., and Biltonen, R. L. (1995) Modulation of phospholipase A_2. Identification of an inactive membrane-bound state, *Biochemistry 34*, 14829−14828.
25. Jain, M. K., and Berg, O. G. (2006) Coupling of the *i*-face and the active site of phospholipase A_2 for interfacial activation, *Curr. Opin. Chem. Biol. 10*, 473−479.
26. Tatulian, S. A., Qin, S., Pande, A. H., and He, X. (2005) Positioning membrane proteins by novel protein engineering and biophysical approaches, *J. Mol. Biol. 351*, 939−947.
27. Pande, A. H., Qin, S., Nemec, K. N., He, X., and Tatulian, S. A. (2006) Isoform-specific membrane insertion of secretory phospholipase A_2 and functional implications, *Biochemistry 45*, 12436−12447.
28. Qin, S., Pande, A. H., Nemec, K. N., and Tatulian, S. A. (2004) The N-terminal α-helix of pancreatic phospholipase A_2 determines productive-mode orientation of the enzyme at the membrane surface, *J. Mol. Biol. 344*, 71−89.
29. Parasassi, T., Krasnowska, E. K., Bagatolli, L., and Gratton, E. (1998) Laurdan and prodan as polarity-sensitive fluorescent membrane probes, *J. Fluoresc. 8*, 365−373.
30. De Vequi-Suplicy, C. C., Benatti, C. R., and Lamy, M. T. (2006) Laurdan in fluid bilayers: Position and structural sensitivity, *J. Fluoresc. 16*, 431−439.
31. Ladokhin, A. S. (1997) Distribution analysis of depth-dependent fluorescence quenching in membranes: a practical guide, *Methods Enzymol. 278*, 462−473.
32. London, E., and Ladokhin, A. S. (2002) Measuring the depth of amino acid residues in membrane-inserted peptides by fluorescence quenching, *Curr. Top. Membr. 52*, 89−115.
33. Qin, S., Pande, A. H., Nemec, K. N., He, X., and Tatulian, S. A. (2005) Evidence for the regulatory role of the N-terminal helix of secretory phospholipase A_2 from studies on native and chimeric proteins, *J. Biol. Chem. 280*, 36773−36783.
34. McIntosh, T. J., and Holloway, P. W. (1987) Determination of the depth of bromine atoms in bilayers formed from bromolipid probes, *Biochemistry 26*, 1783−1788.
35. Nemec, K. N., Pande, A. H., Qin, S., Bieber Urbauer, R. J., Tan, S., Moe, D., and Tatulian, S. A. (2006) Structural and functional effects of tryptophans inserted into the membrane-binding and substrate-binding sites of human group IIA phospholipase A_2, *Biochemistry 45*, 12448−12460.
36. Lakowicz, J. R. (1999) *Principles of Fluorescence Spectroscopy*, 2nd ed., Kluwer Academic/Plenum Publishers, New York.
37. Sturtevant, J. M. (1984) The effects of water-soluble solutes on the phase transitions of phospholipids, *Proc. Natl. Acad. Sci. U.S.A. 81*, 1398−1400.
38. Cevc, G., Ed. (1993) *Phospholipids Handbook*, Marcel Dekker, New York.
39. Böckmann, R. A., Hac, A., Heimburg, T., and Grubmüller, H. (2003) Effect of sodium chloride on a lipid bilayer, *Biophys. J. 85*, 1647−1655.
40. Tatulian, S. A. (1993) Ionization and ion binding, in *Phospholipids Handbook* (Cevc, G., Ed.) pp 511−552, Marcel Dekker, New York.

41. Ladokhin, A. S., Jayasinghe, S., and White, S. H. (2000) How to measure and analyze tryptophan fluorescence in membranes properly, and why bother?, *Anal. Biochem. 285*, 235−245.

42. Cantor, C. R., and Schimmel, P. R. (1980) *Biophysical Chemistry Part II: Techniques for the Study of Biological Structure and Function*, W. H. Freeman and Co., New York.

43. Kung, C. E., and Reed, J. K. (1986) Microviscosity measurements of phospholipid bilayers using fluorescent dyes that undergo torsional relaxation, *Biochemistry 25*, 6114−6121.

44. Upreti, G. C., and Jain, M. K. (1980) Action of phospholipase A_2 on unmodified phosphatidylcholine bilayers: organizational defects are preferred sites of action, *J. Membr. Biol. 55*, 113−121.

BI7015102